Block copolymer films with free interfaces: Ordering by nanopatterned substrates

Xingkun Man and David Andelman[*]

Raymond and Beverly Sackler School of Physics and Astronomy, Tel Aviv University, Ramat Aviv 69978, Tel Aviv, Israel

Henri Orland

Institut de Physique Théorique, CE-Saclay, CEA, F-91191 Gif-sur-Yvette Cedex, France

We study block copolymers (BCPs) on patterned substrates, where the top polymer film surface is not constrained but is free and can adapt its shape self-consistently. In particular, we investigate the combined effect of free interface undulations with wetting of the BCP film as induced by nanopatterned substrates. Under wetting conditions and for a finite volume of BCP material, we find equilibrium droplets composed of coexisting perpendicular and parallel lamellar domains. The self-assembly of BCPs on topographic patterned substrates is also investigated and it is found that the free interface induces mixed morphologies of parallel and perpendicular domains coupled with a nonflat free interface. Our study has some interesting consequences for experimental setups of graphoepitaxy and nanoimprint lithography.

Thin films of block copolymer (BCP) have attracted abiding interest over the years due to their numerous industrial applications, such as for templates and scaffolds for fabrication of nanostructured materials, where many of the essential attributes of photolithography including pattern perfection, registration, and arbitrarily shaped geometries can be reproduced on the nano scale. As such, it has been considered as a legitimate next-generation microelectronics lithography technique for insertion at sub-22-nm technology nodes [1,2].

When thin films of BCP are produced, they self-assemble into ordered nanostructures with a characteristic length scale in the 10- to 100-nm range. Such self-assembled structures mainly depend on chain architecture, film thickness, and surface interactions. In many theoretical studies [3–5] the BCP films are taken to be bound between two flat solid surfaces, and the film structure is influenced by surface interactions and the constrained film thickness. However, in experiments [6–8] the BCP film is spin-cast from solution, and after solvent evaporation, the film is bound only by the bottom substrate, while the top is a free interface with air (vapor). Because the film can locally adjust its height, new phases, which cannot be found when the film is confined between two planar surfaces, can emerge. For example, terrace formation has been found in lamellar [6] and cylindrical BCP thin films [7,8].

In recent experiments [9–15] employing chemically and topographically patterned surfaces with preferential local wetting properties toward one of the two polymer blocks resulted in a unique organization of BCP thin films, as inspired by the demands of the microelectronic industry. In order to have an easily implemented and low-cost technique, the typical length scale of the patterns has to be much larger than the BCP natural periodicity, l_0. However, such a sparse arrangement of stripes results in additional complications as the free interface starts to undulate and may even change the film morphology in ways that are only poorly understood at present.

The aim of this paper is to study the complex and interesting interplay between the BCP/air free interface and nanopatterned substrates. More specifically, we address theoretically this coupling effect on the self-assembly of BCP films using self-consistent field theory (SCFT) and find a strong correlation between the ordering induced by the substrate and the interface profile. Depending on the patterned substrate, we find an undulating free interface or droplet formation, even under *complete wetting* conditions.

In most calculations [3–5] the interface is modeled by a fixed boundary condition. In these cases, such an adjustment of the thickness of the BCP layer with respect to the BCP ordering cannot take place, resulting in a very different ordering. To circumvent this difficulty, we model the BCP film using SCFT adapted for the free interface case [16–20]. The system is composed of polymer chains and a bad solvent (air) inside a fixed volume V. The average BCP volume fraction is $\Phi_P = \Phi_A + \Phi_B$, where Φ_A and Φ_B are the average volume fractions of the two blocks. In order to model a strong phase separation between the polymer and its vapor (air), we add second and third virial terms to the system free energy: $-\frac{1}{2}v\phi_P^2(\mathbf{r}) + \frac{1}{3}w\phi_P^3(\mathbf{r})$, where $\phi_P(\mathbf{r})$ is the local volume fraction of the polymer. For $v > 0$ (bad solvent), the system will undergo demixing and a third virial term with $w > 0$ is needed as a stabilizing term. The two coexisting phases are a polymer-rich phase with $\Phi_P^* \approx v/w$ and a vapor-rich phase, $\Phi_P^* \ll 1$. In all calculations hereafter, we choose $v = 2.6$ and $w = 1.8$. The resulting two-dimensional free energy is then:

$$\frac{b^2 F}{k_B T} = \int d^2\mathbf{r} \left[\chi_{AB}\phi_A(\mathbf{r})\phi_B(\mathbf{r}) - \frac{\Phi_P}{N} \ln Q_c \right.$$
$$- \omega_A(\mathbf{r})\phi_A(\mathbf{r}) - \omega_B(\mathbf{r})\phi_B(\mathbf{r})$$
$$\left. - \frac{v}{2}(\phi_A(\mathbf{r}) + \phi_B(\mathbf{r}))^2 + \frac{w}{3}(\phi_A(\mathbf{r}) + \phi_B(\mathbf{r}))^3 \right]$$
$$- b \int dx [\Delta u_A \phi_A(x,0) + \Delta u_B \phi_B(x,0)] \quad (1)$$

The Flory-Huggins parameter χ_{AB} represents the interaction between the A and the B blocks, $\omega_j(\mathbf{r})$, $j = $ A,B, are the two auxiliary fields coupled with $\phi_j(\mathbf{r})$, and Q_c is the single-chain partition function in the presence of the ω fields. The two
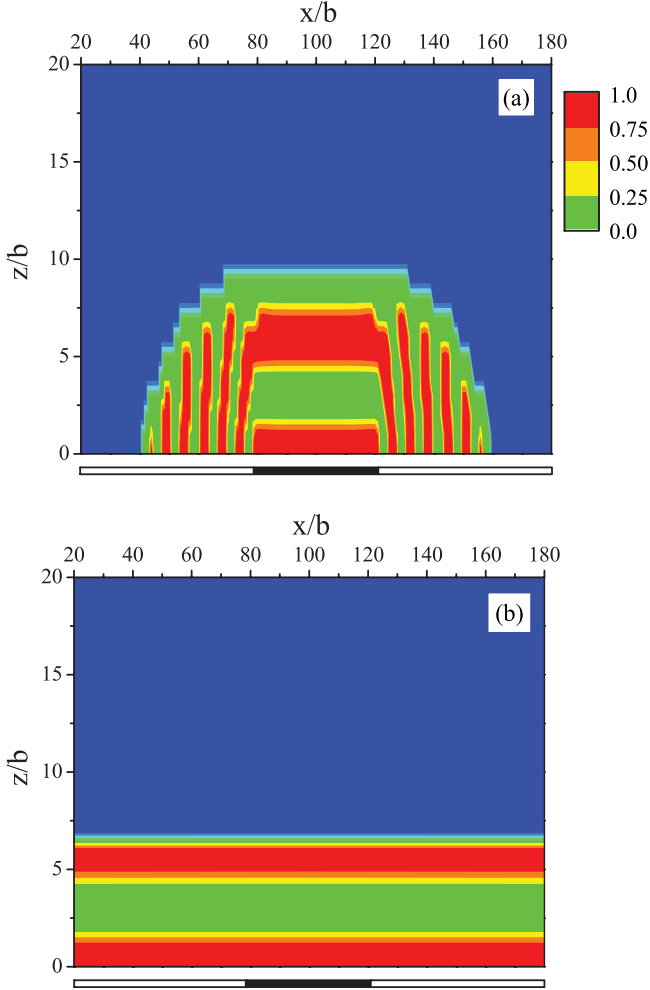
————
[*]andelman@post.tau.ac.il

FIG. 1. (Color online) Contour plots of ϕ_A in the lamellar BCP phase with $N\chi_{AB} = 26$ in contact with a chemically patterned surface. For the middle surface stripe (black) the width is $l_s = 40b$ and $\Delta u_A = 0.6$ and $\Delta u_B = 0.4$, while for the rest of the substrate (white) $\Delta u_A = \Delta u_B = 0.4$. The size of the calculation box is $L_x \times L_z = 200b \times 40b$ and $l_0 \simeq 7b$. (a) $\Phi_P = 0.1$ and the average film thickness is $h_0 \approx 0.6l_0$. (b) $\Phi_P = 0.175$ and the average film thickness $h_0 \approx l_0$. Values of the color code vary between 0 and 1. The air is defined operationally in regions where the total polymer density is <0.05 and is represented by the dark blue (black) color. Only part of the calculation box is shown; note the different scales of the x and z axes.

FIG. 2. (Color online) Contour plots of ϕ_A in the lamellar BCP phase with fixed $\Phi_P \simeq 0.15$, $l_0 \simeq 7b$, and $N\chi_{AB} = 26$ (below ODT). (a) Two chemical surface stripes (black) have a width of $l_s = 20b$, with $\Delta u_A = 0.6$ and $\Delta u_B = 0.4$, while the rest of the surface (white) is neutral, with $\Delta u_A = \Delta u_B = 0.4$. The interstripe region has a width of $l_n = 40b$. (b) Same film as in (a) but with the larger inter-stripe distance of $l_n/b = 80$. The size of the calculation box is $L_x \times L_z = 160b \times 40b$ in (a) and $L_x \times L_z = 200b \times 40b$ in (b). Color code and height of the plotted box are the same as in Fig. 1.

surface parameters are $\Delta u_A = u_A - u_S$ and $\Delta u_B = u_B - u_S$, where u_A, u_B, and u_S represent the short-range interaction of the substrate with the A block, B block, and vapor, respectively. All lengths are expressed in terms of b, the Kuhn length, k_B is the Boltzmann constant, and T is the temperature. For simplicity, each of the BCP chains consists of $N = N_A + N_B$ monomers and is symmetric with $N_A = N_B$.

Using the saddle-point approximation, we obtain a set of self-consistent equations that are solved numerically. As known from previous works [21–23], symmetric BCP in the bulk have a transition between a disordered phase above the order-disorder temperature (ODT), $N\chi_c \simeq 10.5$, and a lamellar phase of natural periodicity l_0, below the ODT. The numerical procedure, i.e., starting with an initial profile and iterating until convergence, allows us to determine
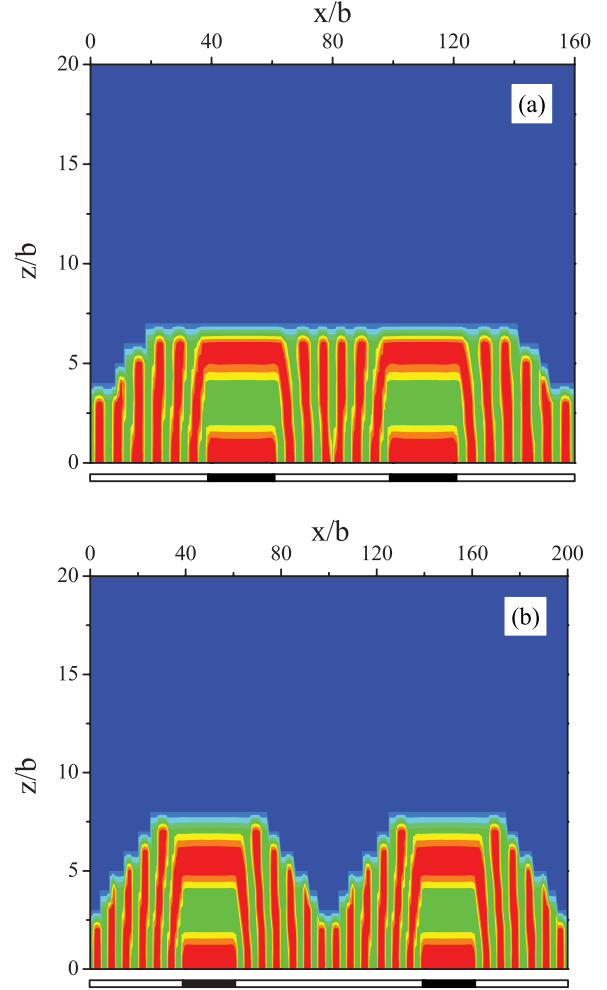
self-consistently the morphological changes inside the BCP film as well as the structure of the nonflat BCP/air interface. Note that, due to the existence of many metastable states, the converged state may strongly depend on the initial conditions.

We first present some results on the adsorption of BCP films on chemically patterned substrates under complete wetting conditions. The BCP film is spread on top of a planar solid substrate modeled as a series of chemical stripes of width l_s and interstripe separation l_n. All stripes have a constant preference for the A block, e.g., $\Delta u_A = 0.6$, $\Delta u_B = 0.4$, while interstripe regions are taken to be neutral, e.g., $\Delta u_A = \Delta u_B = 0.4$. It can easily be seen that this corresponds to complete wetting conditions for both blocks as shown in Fig. 1(b). The figure shows that for our chosen system parameters, the BCP film completely wets the substrate in the case where the film thickness is commensurate with the natural period of the BCP, l_0.
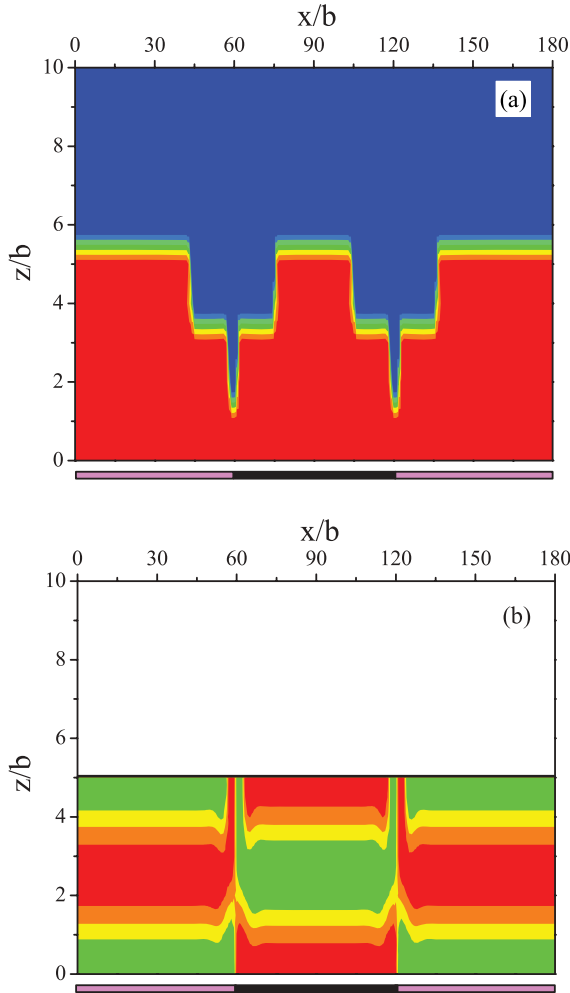
FIG. 3. (Color online) Lamellar BCP structures with a fixed total BCP volume fraction $\Phi_P = 0.12$, $l_0 \simeq 7b$, and $N\chi_{AB} = 26$ (below ODT). (a) Polymer profile ϕ_P is shown. Two chemical stripes of width $l_s = 60b$ and $u_A = 0.4$ and $u_B = 0.6$ are separated by a central stripe (black) of width $l_s = 60b$ and $u_A = 0.6$ and $u_B = 0.4$. (b) For comparison, in the A-block profile ϕ_A is shown for a planar BCP film bound by two solid and flat surfaces at $z = 0$ and $z = 5b$. The patterned substrate and all other parameters are the same as in (a). The size of the calculation box is $L_x \times L_z = 180b \times 40b$ in (a) and $L_x \times L_z = 180b \times 5b$ in (b). Color code is the same as in Fig. 1.

For the case of a single stripe in the center of a large substrate, although we are under wetting conditions, a BCP droplet can be obtained [Fig. 1(a)]. We choose an amount of BCP such that its homogeneous spreading over the entire substrate is equal to a noninteger number of parallel lamellae, $h_0 = 0.6l_0$. Starting from a localized "rectangular"-shaped lamellar BCP droplet as an initial condition, after convergence we obtain a BCP droplet residing on the substrate as shown in Fig. 1(a). It is composed of coexisting perpendicular and parallel lamellae in registry with the patterned substrate. The free-energy density of this droplet is $f = -0.0535$. In contrast, when the initial condition is taken to be a flat BCP film above its ODT, a parallel lamellar phase is obtained with free energy density $f = -0.0520$, clearly larger than that of the droplet. The droplet shown in Fig. 1(a) is more stable because the parallel domain height is larger than h_0 as it tries
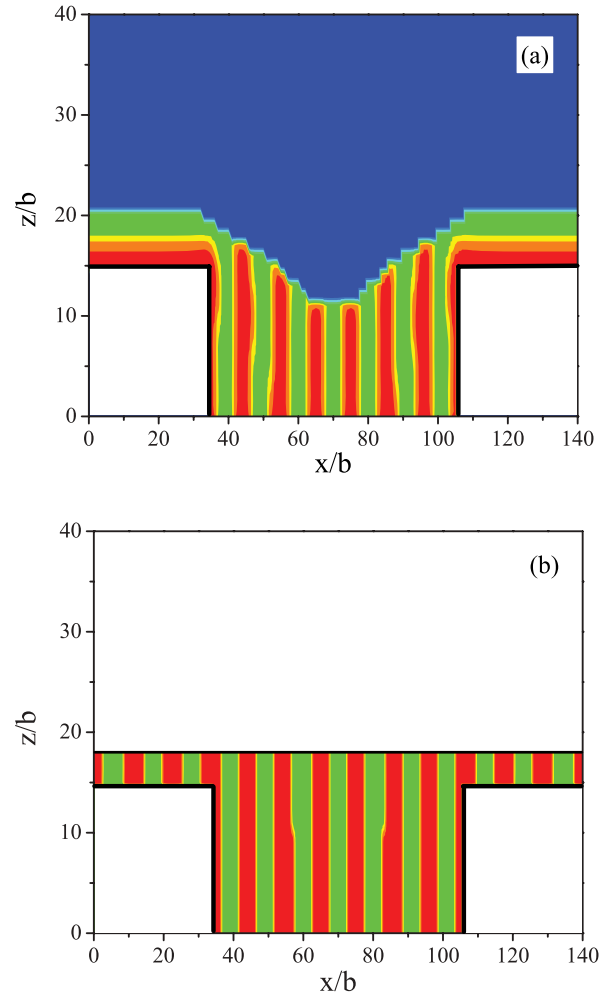

FIG. 4. (Color online) BCP lamellar structures for topographical surfaces (grooves) with $\Phi_P \simeq 0.32$, $l_0 \simeq 10b$, and $N\chi_{AB} = 43.2$. (a) Contour plot of the A block, ϕ_A. $\Delta u_A = 0.12$ and $\Delta u_B = 0.1$ for the vertical and side walls, while $\Delta u_A = \Delta u_B = 0.1$ for the bottom of the groove. (b) The BCP is bound from above by a second solid surface, leading to a perfect perpendicular orientation. All other parameters are the same as in (a). Color code is the same as in Fig. 1.

to accommodate an integer number of layers. Consequently, as the BCP volume is fixed, the height of these perpendicular domains should compensate that of the parallel ones.

In certain cases the lamellar phase can be the more stable one [Fig. 1(b)]. Performing the same set of calculations as above with an amount of BCP corresponding to one lamellar period, $h_0 = l_0$, we find that the lamellar phase has a free energy density $f = -0.0998$ and is more stable than that of the droplet with $f = -0.0957$.

It is natural to generalize the results in Fig. 1 to more than one surface stripe. An undulating BCP/air interface in this case follows in registry the stripe structure of the surface. This is shown in Fig. 2, where the substrate has two chemical stripes. Because different surface regions induce parallel and perpendicular lamellae structures, their coexistence yields an undulating BCP/air interface [Fig. 2(b)]. Moreover, we find that the undulating free interface depends on the interstripe distance l_n. If l_n becomes small [24], the BCP/air interface between the two stripes is almost flat [Fig. 2(a)]. This means

that the stripes cannot be too sparse (as desired in many applications) if one wants to obtain a flat free interface.

Further difference between the free interface and the flat (and rigid) interface can be seen in Fig. 3. The patterned surface is chosen with alternating stripes preferring A and B layers inducing parallel lamellar domains. As shown in Fig. 3(a), the overall polymer profile $\phi_P(\mathbf{r})$ displays several terraces at the free interface. They are induced by defects in the film [not shown in Fig. 3(a)], which are themselves created because of the patterned substrate. The terraces are in registry with the substrate stripe boundaries and the jumps in the terrace height correspond to half of the lamellar periodicity. The situation is rather different in Fig. 3(b), where the top interface is forced to be planar. The film has the same total volume as in Fig. 3(a), yielding a constant height $h_0 = 5b$. However, differences in the A-block profile, ϕ_A, as induced by the surface stripes preferring the A or B lamellae are clearly shown.

We also considered the situation where BCP films are in contact with topographic patterned substrates used in graphoepitaxial [12,13,25] and nanoimprint lithography [14,15,26,27] setups. The surface is modeled as a sequence of grooves that have a slight preference toward one of the blocks (say, the A block). When the BCP volume exceeds the inner volume of the groove, we obtain a mixed state composed of parallel and perpendicular lamellar domains [Fig. 4(a)]. One of our conclusions is that a perfect perpendicular lamellae structure can be obtained when the BCP is bounded by a top flat solid surface, as shown in Fig. 4(b). This suggests that pressing the film between the grooved mold and a second solid surface facilitates the formation of a perpendicular lamellar orientation and is superior to the free interface setup, as in Fig. 4(a).

In this paper we have addressed the combined effects of nanopatterned substrates and the polymer/air free interface on the self-assembly of BCP thin films. We have treated air as a bad solvent and modified the SCFT accordingly in order to study the phase behavior of finite-volume films. We obtained an undulating polymer/air interface when the films are casted on chemically patterned substrates. For a sequence of chemical stripes, we find that the undulations of the BCP/air interface depend on the interstripe spacing. In particular, by adjusting the substrate affinity, we can obtain BCP droplets containing mixed perpendicular and parallel lamellae. We also studied the self-assembly of BCP thin films on topographic substrates. If the BCP amount exceeds the groove inner volume, we obtain a mixed perpendicular and parallel lamellar structure instead of a perfect two-dimensional perpendicular lamellae. Furthermore, we find that it is more efficient to confine a BCP film between a solid mold and a counter planar surface in order to obtain a perfect perpendicular lamellar structure.

Our SCFT calculations show new and interesting phases of BCP thin films where the free interface displays height variations coupled with morphological changes as determined by the patterned substrate. Even small height variations allow the relaxation of the frustration due to the incompressibility of the BCP lamellae, in contrast to fixed boundary models, leading to BCP ordering that is very different in these two approaches. We, finally, note that the polymer-vapor interaction parameter is chosen as $\nu = 2.6$, while the AB interfacial tension varies between $\chi_{AB} = 1.3$ (Figs. 1–3) and 0.8 (Fig. 4). This means that the magnitude of χ_{AB} is not much smaller than ν as is the case for typical BCP systems. For example, for polystyrene (PS) and poly(methyl methacrylate) (PMMA) used in Ref. [20], the surface tension with the air is 31.2 and 31.4 dyne/cm), while the PS-PMMA interfacial tension is about 1.5 dyne/cm (in the proper temperature range). Unfortunately, such an extreme tension ratio, $\chi_{AB} \ll \nu$, is troublesome for the SCFT calculation, because much finer grids are required at larger ν values. The same numerical difficulty has also been reported in Ref. [20].

We hope that, in the future, more numerically intensive calculations for free interfaces will shed additional light on the phase behavior of BCP thin films as influenced by their nanopatterning substrates and free interfaces.

[1] W.-K. Li and S. Yang, J. Vac. Sci. Technol. B **25**, 1982 (2007).

[2] In International Technology Roadmap for Semiconductors (ITRS), 2009 ed.; available at: http://www.itrs.net.

[3] M. W. Matsen, J. Chem. Phys. **106**, 7781 (1997).

[4] D. Petera and M. Muthukumar, J. Chem. Phys. **109**, 5101 (1998).

[5] Y. Tsori and D. Andelman, J. Chem. Phys. **115**, 1970 (2001).

[6] G. Coulon, T. P. Russell, and V. R. Deline, Macormolecules **22**, 2581 (1989).

[7] A. Knoll, A. Horvat, K. S. Lyakhova, G. Krausch, G. J. A. Sevink, A. V. Zvelindovsky, and R. Magerle, Phys. Rev. Lett. **89**, 035501 (2002).

[8] A. Knoll, R. Magerle, and G. Krausch, J. Chem. Phys. **120**, 1105 (2004).

[9] M. Stoykovich, M. Müller, S. Kim, H. Solak, E. Edwards, J. J. de Pablo, and P. F. Nealey, Science **308**, 1442 (2005).

[10] R. Ruiz, H. M. Kang, F. A. Detcheverry, E. Dobisz, D. S. Kercher, T. R. Albrecht, J. J. de Pablo, and P. F. Nealey, Science **321**, 936 (2008).

[11] J. Bang, U. Jeong, D. Y. Ryu, T. P. Russell, and C. J. Hawker, Adv. Mater. **21**, 4769 (2009).

[12] R. Segalman, H. Yokoyama, and E. J. Kramer, Adv. Mater. **13**, 1152 (2001).

[13] G. E. Stein, W. B. Lee, G. H. Fredrickson, E. J. Kramer, X. Li, and J. Wang, Macromolecules **40**, 5791 (2007).

[14] H.-W. Li and W. T. S. Huck, Nano Lett. **4**, 1633 (2004).

[15] V. Voet, T. Pick, S.-M. Park, M. Moritz, A. Hammack, D. Urban, D. Ogletree, D. Olynick, and B. Helm, J. Am. Chem. Soc. **133**, 2812 (2011).

[16] M. Müller and L. G. MacDowell, Macromolecules **33**, 3902 (2000).

[17] K. Kargupta and A. Sharma, Phys. Rev. Lett. **86**, 4536 (2001).

[18] H. Morita, T. Kawakatsu, and M. Doi, Macormolecules **34**, 8777 (2001).

[19] K. S. Lyakhova, A. Horvat, A. V. Zvelindovsky, and G. J. A. Sevink, Langmuir **22**, 5848 (2006).

[20] U. Kim and M. W. Matsen, Soft Matter **5**, 2889 (2009).

[21] L. Leibler, Macromolecules **13**, 1602 (1980).

[22] M. W. Matsen and M. Schick, Phys. Rev. Lett. **72**, 2660 (1994).

[23] X. K. Man, D. Andelman, and H. Orland, Macormolecules **43**, 7261 (2010).

[24] Numerically we determine that the critical value of l_n is around $6l_0$, namely, when $l_n \leqslant 6l_0$ we can only obtain a flat interface between two stripes, as shown in Fig. 2(a).

[25] R. Mukherjee, D. Bandyopadhyay, and A. Sharma, Soft Matter **4**, 2086 (2008).

[26] X. K. Man, D. Andelman, H. Orland, P. Thébault, P.-H. Liu, P. Guenoun, J. Daillant, and S. Landis, Macromolecules **44**, 2206 (2011).

[27] P. Thebault, S. Niedermayer, S. Landis, N. Chaix, P. Guenoun, J. Daillant, X. K. Man, D. Andelman, and H. Orland, Adv. Mater. **24**, 1952 (2012).